Use of Kramers–Kronig transforms for the treatment of admittance spectroscopy data of *p*-*n* junctions containing traps

C. León, J. M. Martin, and J. Santamaría
Departamento de Física Aplicada III, Facultad de Ciencias Físicas, Universidad Complutense, 28040 Madrid, Spain

J. Skarp
Microchemistry LTD, Keilaranta 6, SF 02151, Espoo, Finland

G. González-Díaz and F. Sánchez-Quesada
Departamento de Física Aplicada III, Facultad de Ciencias Físicas, Universidad Complutense, 28040 Madrid, Spain

(Received 5 July 1995; accepted for publication 29 January 1996)

The use of Kramers–Kronig transforms is proposed for the treatment of admittance spectroscopy data of junctions when significant shunt conductance or series resistance is present. An algorithm has been implemented to calculate the transformations numerically and the validity of the method developed has been tested using simulated data. Two experimental systems, *p*-*n* junctions into InP made by ion implantation, and atomic-layer-epitaxy-grown CdS/CdTe heterojunctions, have been characterized using this procedure. © *1996 American Institute of Physics.*
[S0021-8979(96)08909-2]

I. INTRODUCTION

Deep impurity levels are responsible for major properties in semiconductor devices. Deep level transient spectroscopy (DLTS) is the most extended method to characterize them, although admittance spectroscopy (AS) is an alternative technique especially useful for detecting relatively fast (or shallow) levels. AS, as developed by Losee[1] and further developed theoretically by Pautrat *et al.*[2] and Ghezzi,[3] consists of measuring the junction admittance as a function of temperature and frequency. While AS is usually conducted measuring small-signal admittance at a few discrete frequencies sweeping the temperature over the required range, another possibility is to sweep the frequency for a few fixed temperatures. Both methods are equivalent, and the choice between them depends only on the experimental setup available. Deep levels crossing the Fermi level give rise to a relaxation in the capacitance when the frequency of the ac signal or the temperature are changed in the proper range. The application of a small ac voltage causes a charge oscillation arising from trapping and detrapping of carriers around the point where the Fermi level crosses the trap. This contributes to the junction capacitance as far as the frequency is lower than the inverse of the proper time of the trap (directly related to emission and capture rates). At this critical frequency the mentioned relaxation occurs causing a decrease in the real part of the capacitance C' and a peak in the imaginary part C''. The peak frequency ω_p can be related to the energy position of the trap through the following equation:

$$\omega_p = N_B \nu_{\mathrm{th}} \sigma \exp(-\Delta E/kT), \tag{1}$$

where σ is the capture cross section, v_{th} is the thermal velocity, N_B is the effective density of states of the band, and ΔE is the energy position of the trap in the gap.

Although a Debye-like relaxation is obtained for the complex junction capacitance solving the detailed balance equation for the trap in a small signal approach, significant departures from the Debye behavior have been observed probably obeying spatial or energy distribution of traps. On the other hand, various factors such as shunt conductance or series resistance can seriously distort the peak due to the deep level or even make it disappear. This is because the contribution to the conductance due to deep levels is usually low and a relatively low shunt conductance can easily overshadow it. Series resistance involves an additional relaxation in the capacitance but in most cases it occurs at frequencies high enough to show no effect on measured data. The presence of shunt conductance or series resistance can also make the peak shift in frequency, leading then to wrong results. Real capacitance data can be easily corrected for series resistance and, as shown below, they are not affected by shunt conductance, so that information about traps can be obtained from it using the Kramers–Kronig transforms. This procedure can be avoided by a complex nonlinear least-squares fitting to a response model describing the relaxation;[4–6] however, when dealing with experimental data the model is often unknown, i.e., no analytical expressions nor equivalent electrical circuits are known to obtain the distribution of relaxation times. In this sense, the use of Kramers–Kronig transforms to obtain the imaginary part of the junction capacitance is a straightforward way to determine the energy position of the trap.

This work presents the use of Kramers–Kronig (KK) relations between real and imaginary components of the capacitance to obtain the peak associated with a deep level free of the influence of the factors explained above. It is based on the fact that the real part of the capacitance is not influenced by the shunt dc conductance. Since the KK relations are computed in the frequency domain, the frequency-swept technique has to be used in order to apply the method proposed here. Some authors have previously used the Kramers–Kronig relations in electrochemical studies and in

 0021-8979/96/79(10)/7830/7/$10.00 © 1996 American Institute of Physics

impedance spectroscopy data analysis.[7–9] These relations are usually employed to show the validity of experimental admittance data or to study linearity and stability of systems. We have developed a computer routine to evaluate the integrals involved in KK relations. Some relevant aspects of this program concerning the proper evaluation of these integrals are explained. Simulations of admittance data are used to check the validity of the method and some of them are presented. Finally, we demonstrate the usefulness of the method developed by applying it in the analysis of admittance data of InP *p-n* junctions and a CdTe/CdS solar cell.

II. METHOD AND APPLICATION TO SIMULATED DATA

Junction admittance $Y(\omega)$ is defined as the relation between electric current and the applied electric voltage,

$$I(\omega)=Y(\omega)V(\omega). \tag{2}$$

For the purpose of this work a complex capacitance C^* is introduced defined as

$$C^*(\omega)=\frac{Y(\omega)}{j\omega}, \tag{3}$$

which can be written in terms of its real and imaginary parts as

$$C^*(\omega)=C'(\omega)-jC''(\omega). \tag{4}$$

Both components of complex capacitance are obtained from AS measurements, and can be expressed in terms of an equivalent dielectric susceptibility, a more general function, as

$$C'(\omega)=k\epsilon_0[1+\chi'(\omega)], \tag{5}$$

$$C''(\omega)=k\left(\frac{\sigma_0}{\omega}+\epsilon_0\chi''(\omega)\right), \tag{6}$$

where k is a pure geometrical factor, ϵ_0 the vacuum permittivity, and σ_0 is the dc conductivity.

Real and imaginary components of the susceptibility are related by the Kramers–Kronig relations by the following expressions:[10]

$$\chi'(\omega)=\frac{2}{\pi}\int_0^\infty \frac{x\chi''(x)}{x^2-\omega^2}\,dx, \tag{7}$$

$$\chi''(\omega)=-\frac{2}{\pi}\int_0^\infty \frac{\omega\chi'(x)}{x^2-\omega^2}\,dx, \tag{8}$$

derived as a pure mathematical result, provided the following four general requirements are fulfilled: causality, (the response of the system must be only due to the applied perturbation); linearity (the response of the system must be independent of the magnitude of the perturbation); stability (system must return to its original state after the perturbation is removed); Continuity (susceptibility must be continuous and finite valued for all frequencies and finite valued at the limits $\omega\rightarrow 0$ and $\omega\rightarrow\infty$).

The program written to evaluate numerically the integrals involved in KK relations and to obtain the imaginary (or real) part of capacitance from the real (or imaginary) part uses as input data a set of complex capacitance values measured at discrete frequencies over a range of a few decades (usually 20 Hz–1 MHz). The output data can be obtained at any desired frequency in the measuring interval.

Numerical integration of any of the KK relations requires the knowledge of the susceptibility function in the whole frequency spectrum, however, the measured data are a discrete and finite set. This problem is approximately solved with the algorithm used from which the following aspects should be underlined:

(i) Since the experimental frequency window is finite, the contribution of lower and higher frequencies to the integral cannot be taken into account. (This is known as the tails problem.) Measured data have been extrapolated by one decade beyond the measuring frequency edges to improve the results of integration. A linear least-squares fit of one decade at the edges of the measuring frequency range is used to do a linear extrapolation in a double logarithmic scale. This is usually enough as far as the numerator under the integral is a slowly varying function of frequency at the edges of frequency window, and provided the denominator is a rapidly growing function of the difference between frequencies considered.

(ii) Another problem is not having an analytic expression for the frequency dependence of the susceptibility in the range of integration to obtain its value numerically. It is thus necessary to interpolate for creating a curve between experimental data. Since usually susceptibility is a slowly varying function with frequency in a log–log scale, a two-degree polynomial function between each three data points can be used to interpolate with enough accuracy if logarithmic values are being used. We have used the Aitken[11] method to interpolate because it does not require the points to be equally spaced in frequency.

Another point that should be underlined when evaluating the integral is that the denominator becomes zero at $x=\omega$. This singularity is avoided separating the total integration interval into three subintervals,

$$\frac{\omega_i}{10}<x<10^{-1/\mathrm{ppd}}\omega=i, \tag{9}$$

$$10^{-1/\mathrm{ppd}}\omega=i<x<10^{1/\mathrm{ppd}}\omega=s, \tag{10}$$

$$10^{1/\mathrm{ppd}}\omega=s<x<10\omega_f, \tag{11}$$

where ω_i and ω_f are the first and last frequencies of the experimental window, and ppd is the number of points per decade selected to do the transformation. Even if the measuring points are not equispaced in frequency the interpolation mentioned allows calculating the integral at frequency points spaced by 1/ppd in a log scale. This permits defining an arbitrarily narrow interval, limited by i and s, around the frequency at which the integral is being calculated (ω).

For the first and last subintervals, integration has been performed simply by using Simpson's rule.[11] Integrating by parts and assuming the susceptibility to behave linearly between i and s, the integral in the central subinterval may be approximated by the following expressions:

$$\frac{2}{\pi}\int_i^s \frac{\omega\chi'(x)}{x^2-\omega^2}\,dx$$

$$=\frac{1}{\pi}\left[\frac{\chi'(s)-\chi'(i)}{s-i}\,\omega\,\ln\left(\frac{s^2-\omega^2}{\omega^2-i^2}\right)\right.$$

$$\left.+\frac{\chi'(i)s-\chi'(s)i}{s-i}\ln\left(\frac{(s-\omega)(\omega+i)}{(s+\omega)(\omega-i)}\right)\right], \qquad (12)$$

$$\frac{2}{\pi}\int_i^s \frac{x\chi''(x)}{x^2-\omega^2}\,dx$$

$$=\frac{2}{\pi}[\chi''(s)-\chi''(i)]$$

$$+\frac{1}{\pi}\left[\frac{\chi''(s)-\chi''(i)}{s-i}\,\omega\,\ln\left(\frac{(s-\omega)(\omega+i)}{(s+\omega)(\omega-i)}\right)\right.$$

$$\left.+\frac{\chi''(i)s-\chi''(s)i}{s-i}\ln\left(\frac{s^2-\omega^2}{\omega^2-i^2}\right)\right]. \qquad (13)$$

This procedure facilitates the numerical integration around $x=\omega$ providing analytical expressions of the integrals in this interval and is shown to work satisfactorily as discussed below. A different integration procedure has been proposed by other authors.[9]

The validity of the method was tested using two different simulated systems. Both sets of data were generated from 100 Hz to 1 MHz with 10 points per decade.

The first, shown in Fig. 1(a), represents a system with a Debye-like dielectric relaxation and a superimposed shunt dc conduction. A Debye-type relaxation is characterized by a single relaxation time τ and therefore complex capacitance is given by the expression

$$C^*(\omega)=C_\infty+\frac{C_0-C_\infty}{1+j\omega\tau}-j\,\frac{G_0}{\omega}, \qquad (14)$$

where C_0 and C_∞ denotes the constant values of the real part at low and high frequencies, respectively, and G_0 is the shunt conductance. We have chosen $C_0=20$ pF, $C_\infty=10$ pF, $\tau=10^{-5}$ s, and $G_0=10^{-6}$ S for the simulation. This system satisfies all conditions listed above and C' is practically constant at the limits of the frequency window. Therefore, there must not be any significant deviation in C'' between simulated data and data obtained through KK relations. In fact, the simulated imaginary capacitance data after removing dc conduction and those obtained KK transforming the real simulated data differ in less than 1% for three decades in frequency around the peak and only small departures are found at the high-frequency edge due to the tails problem already mentioned. Data are presented in Fig. 1(b).

The second simulation [Fig. 2(a)] represents a system with a Cole–Cole dielectric relaxation and a dc conduction. The complex capacitance is given by the expression

$$C^*(\omega)=C_\infty+\frac{C_0-C_\infty}{1+(j\omega\tau)^\alpha}-j\,\frac{G_0}{\omega}, \qquad (15)$$

where α accounts for a distribution of relaxation times and satisfies $0<\alpha<1$. The parameters for the simulation have been $C_0=20$ pF, $C_\infty=10$ pF, $\tau=10^{-5}$ s, $\alpha=0.6$, and

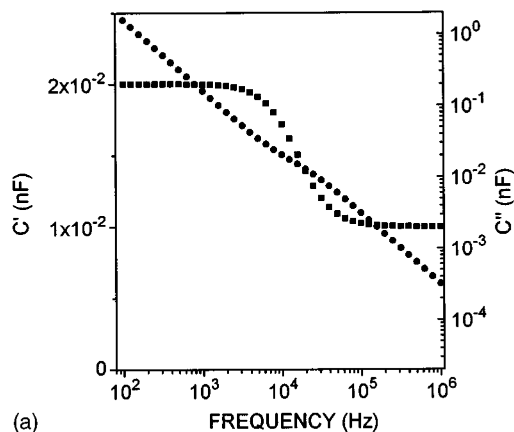

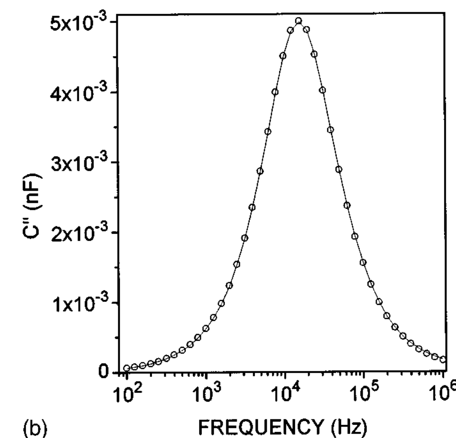

FIG. 1. (a) C' (■) and C'' (●) for a simulated system showing a Debye dielectric relaxation and a superimposed shunt dc conduction according to expression (14). The parameters chosen for the simulation were $C_0=20$ pF, $C_\infty=10$ pF, $\tau=10^{-5}$ s, and $G_0=10^{-6}$ S. (b) C'' for the previous system without shunt dc conduction (○). Solid line represents C'' obtained from C' data using KK relations.

$G_0=10^{-6}$ S. In a Cole–Cole relaxation the peak is wider and real and imaginary parts of the complex capacitance decrease as $\omega^{-\alpha}$ at high frequencies; this behavior commonly appears in p-n junctions containing traps. This response is usually explained in terms of a continuous energy distribution of traps states or of a spatial distribution of a single trap level. As in the first simulation, we have also plotted the imaginary simulated data after removing dc conduction and the imaginary data obtained from KK transforms of the real simulated data [Fig. 2(b)]. This system exhibits a stronger variation of C' near the edges of the frequency window. This involves that extrapolated values are poorer and, consequently, the tails problem becomes more critical. Nevertheless, the difference is below 1% for one frequency decade at each side of the maximum, being this enough to correctly define the shape of the peak. In order to show that the origin of the errors at the edges, even for exact synthetic data, is in the extrapolation of C' data, Fig. 2(b) also presents KK transformed C'' using the exact data from expression (15) as extrapolated values for C' beyond the edges of the frequency window. In this case there is no appreciable difference from the exact C'' data from simulation.

Alternative methods to KK transforms for analyzing ad-

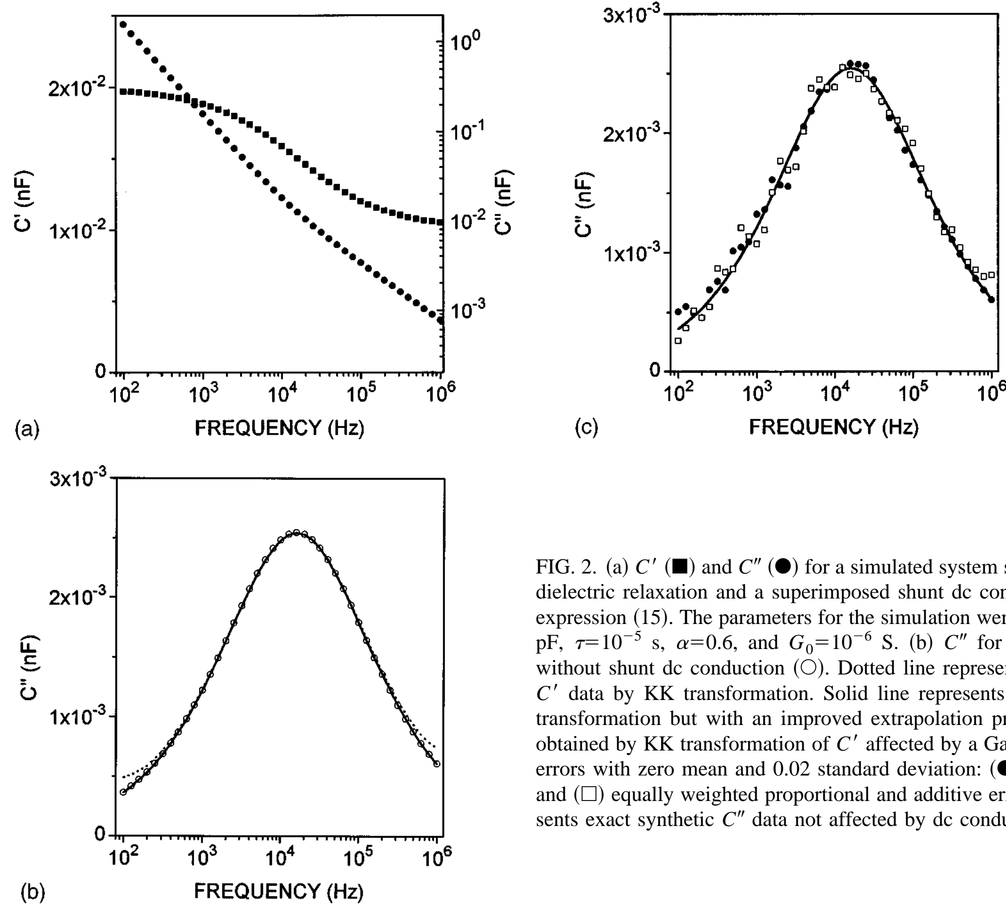

FIG. 2. (a) C' (■) and C'' (●) for a simulated system showing a Cole–Cole dielectric relaxation and a superimposed shunt dc conduction according to expression (15). The parameters for the simulation were $C_0=20$ pF, $C_\infty=10$ pF, $\tau=10^{-5}$ s, $\alpha=0.6$, and $G_0=10^{-6}$ S. (b) C'' for the previous system without shunt dc conduction (○). Dotted line represents C'' obtained from C' data by KK transformation. Solid line represents C'' obtained by KK transformation but with an improved extrapolation procedure. (c) C'' data obtained by KK transformation of C' affected by a Gaussian distribution of errors with zero mean and 0.02 standard deviation: (●) proportional errors and (□) equally weighted proportional and additive errors. Solid line represents exact synthetic C'' data not affected by dc conduction.

mittance spectroscopy data have been proposed recently based on fitting experimental data to a distribution of relaxation times[5,6] which allow obtaining one of the parts of the susceptibility (real or imaginary) from the other avoiding the extrapolation problem. It is worthwhile referring to a very recent approach by Boukamp[12] which uses a linear fit to get an arbitrary number of relaxation time estimates with no iteration. This method shows that the uncertainties in the parameters have virtually no consequences in the susceptibility determination as far as they provide a good fit to the experimental data. Any of those methods should be applicable to analyze the experimental data of p-n devices presented below, however, series or shunt resistances must be treated as separate parameters to avoid confounding their effects with those of the distribution of relaxation times.

The simulations used above confirm the validity of the method with exact synthetic data, but not necessarily with real data which may be affected by experimental errors. The question of the transformation of errors in KK transforms has been already discussed by other authors.[9] Gaussian errors with zero mean and 0.02 standard deviation were used in generating data with either proportional or additive and proportional errors as proposed in Ref. 9. In this way the Cole–Cole relaxation data modified by the presence of random errors have been used to check the validity of the algorithm for ''experimental'' data. Figure 2(c) presents the imaginary part of the complex capacitance obtained from KK transformation of the real part affected by two different kinds of errors: proportional and equally weighted additive and proportional errors. Exact data of the imaginary part of the capacitance not affected by the dc conductance are also plotted in the same figure. It can be seen that the shape and position of the peak are maintained for the transformed data. Since experimental errors are usually smaller than the ones used in these simulations, we can state that the errors present on real data do not pose serious difficulties in analyzing admittance spectroscopy data using KK transforms.

III. EXPERIMENT

The InP p-n junctions were made by ion implantation. Mg was implanted into undoped InP at 80 keV with a dose of 10^{14} cm^{-2}. The undoped InP was n type, with n concentration around 2×10^{15} cm^{-3}. The implanted samples were rapid thermal annealed at 875 °C for 5 or 10 s, which has been measured to produce p-type doping with p around 3×10^{18} cm^{-3}.[13] Ohmic contacts of AuGe/Au (for the n-type zone) and AuZn/Au (for the p-type zone) were deposited by thermal evaporation and subsequent alloying at 420 °C for 1 min. The junctions were defined by the evaporated dots, which were squares of 500×500 μm^2, being isolated from each other by ion implantation. Using the dots as implantation mask, He was implanted at 90 keV with a dose of 10^{14} cm^{-2}. The energy of this implantation was calculated for it to penetrate deeper than the p zone of the junctions, but without passing through the AuZn/Au contacts on the top.

The He implantation into p-type InP is reported to give a resistivity high enough to achieve a good isolation between the diodes.[14]

The CdTe/CdS heterojunctions were grown by atomic layer epitaxy (ALE). The ALE CdS/CdTe thin-film solar-cell structure was simultaneously processed on SnO_2-coated soda lime glass in an ALE reactor type F-120. The thicknesses of CdS and CdTe layers were 100 and 2500 nm, respectively. No intentional dopings of the films were made. The back contact consists of layers of Cu/Ni/Al sputtered on the CdTe surface previously etched with H_3PO_4–HNO_3 acid mixture. More details on the fabrication method can be found in Refs. 15 and 16.

Complex admittance was measured in a Hewlett–Packard 4284A *LCR* meter, in the frequency range 100 Hz–1 MHz, at constant temperatures, from 200 to 330 K. The ac signal was in all cases 50 mV, which gave a stable reading even at low frequencies. The data acquisition was computer controlled, using the IEEE-488 standard. Each recorded measurement was obtained as an average of 16 single measurements, which resulted in very low noise. The samples were mounted on a Cu piece, in which a K-type thermocouple was tightened, using an Ag conductive composite. To avoid oxidation or water condensation on the samples, an inert atmosphere was kept in the measurement cell by using a flux of N_2. All samples were measured in the dark.

IV. RESULTS AND DISCUSSION

The data of the ion-implanted p-n junctions into InP annealed with two different times are shown to illustrate how the effect of the shunt conductance on complex capacitance measurements can be eliminated using the technique explained above, showing the presence of one or more peaks in C'' otherwise overshadowed by it. After that, data of CdTe/CdS heterojunction are used to demonstrate the usefulness of the same technique when the presence of a series resistance introduces a distortion in the form of a peak in C''.

A. InP p-n junctions

Real and imaginary parts of the complex capacitance of an InP p-n junction annealed at 875 °C for 10 s, measured at 273 K, are shown in Fig. 3. The imaginary part of the capacitance C'' obtained from the real one by KK relations is also shown. It can be seen that no peaks appear in the measured imaginary component of the capacitance. This component is dominated by the term G_0/ω due to a significant shunt conductance G_0, resulting in a straight line with slope -1 at low frequencies in the log–log plot. The shunt conductance was found to be due to the isolation implant, as other junctions processed by mesa etching did not show this contribution. Obtaining the true junction C'' by simply subtracting a term of the form G_0/ω (i.e., the shunt conductance) is not possible, since the magnitude of the true C'' may be of the same order of magnitude as the experimental error of the measurement at low frequencies. Since, as explained above, the parallel conductance has no effect on the real part of the capacitance, the trap related peak (see Fig. 3) can be obtained by KK transformation of C'. The traps cannot respond to the ac signal at high frequencies, and C' is due only to oscillations in the width of the depletion region, whereas at sufficiently low frequencies traps response gives rise to an additional contribution in C'.

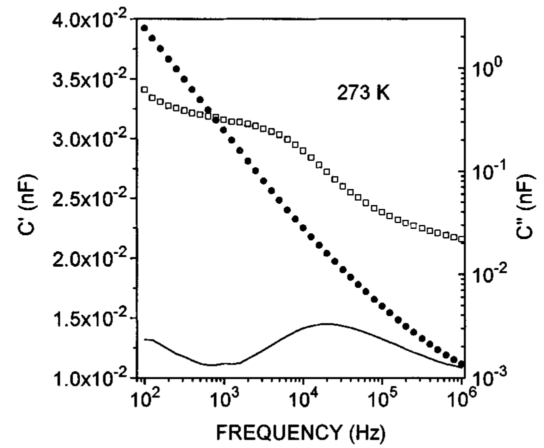

FIG. 3. C' (□) and C'' (●) for an InP p-n junction annealed at 875 °C for 10 s, measured at 273 K. The solid line represents C'' obtained by KK transforms from C'.

Figure 4 shows the complex capacitance of the same sample at four different temperatures. The imaginary parts

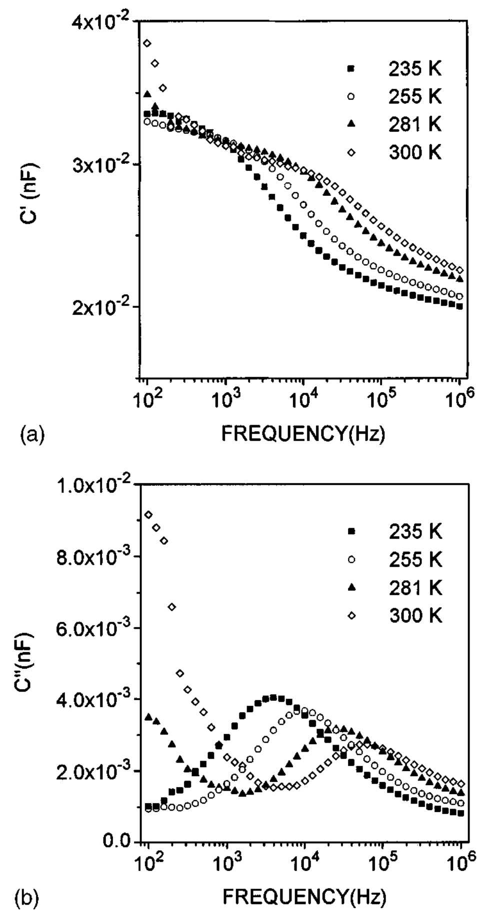

FIG. 4. (a) C' for an InP p-n junction annealed at 875 °C for 10 s, measured at different temperatures. (b) C'' data obtained by KK transforms from the C' data shown in (a).

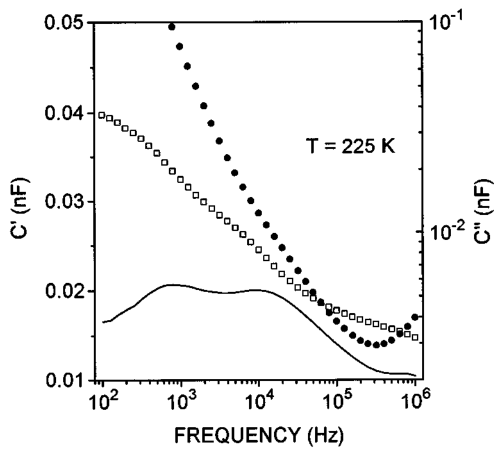

FIG. 5. C' (□) and C'' (●) for an InP p-n junction annealed at 875 °C for 5 s, measured at 225 K. The solid line represents C'' obtained by KK relations from C'.

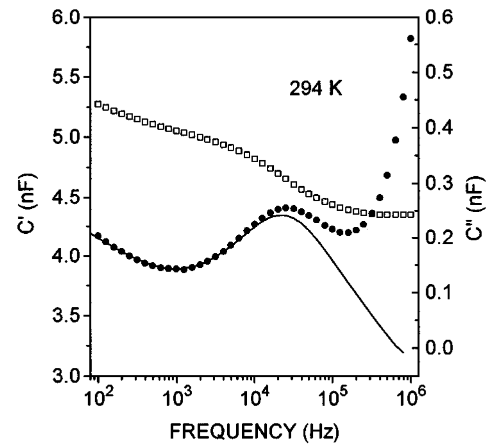

FIG. 6. C' (□) and C'' (●) for a CdS/CdTe heterojunction measured at 294 K. The solid line represents C'' obtained by KK transforms from C'.

were obtained from the real ones using the method described here. The emission rate of traps is related to the peak frequency through the expression quoted in the introduction. A plot of ω_p/T^2 in a logarithmic scale, where T^{-2} accounts for the temperature dependence of the pre-exponential factor, versus the reciprocal temperature, yields a straight line whose slope is directly related to the energy level of the trap. Assuming this model, an activation energy of 0.2 eV has been obtained.

The InP p-n junctions annealed at the same temperature but only for 5 s showed two different peaks as can be seen in Fig. 5. These peaks cannot be directly observed from measured data, again due to a significant shunt conductance, and appear clearly in C'' only when it is obtained via KK relations from C' experimental data. The peak observed in this figure at higher frequencies was found to have an activation energy of 0.2 eV, which seems to indicate that this peak has the same origin as the one found in the sample annealed at 875 °C for 10 s and is probably due to the He implantation.[17] The origin of the second deep level, of activation energy around 0.35 eV, could be related to the implantation damage, as it disappears for anneals with longer times.

B. CdTe/CdS solar cell

AS measurements on the CdTe/CdS heterojunction at 294 K are presented in Fig. 6. It displays the C' and C'' measured, as well as C'' obtained from the C' measured through the KK relations. It is again observed the presence of a deep level giving rise to a relaxation in the capacitance. At this temperature, there is not a significant shunt conductance affecting the measured C'' at low frequencies, but the beginning of a new peak can be seen at high frequencies. It appears as a consequence of a Debye-like relaxation in the capacitance due to the existence of a series resistance R_s. The proper time of this relaxation calculated as the product of R_s (5 Ω, obtained from the $I-V$ characteristics of the cell) and the high-frequency C' ($C'_{\mathrm{hf}} = 4.35$ nF) is 2.18×10^{-8} s, and therefore the relaxation occurs at $1/2\pi\tau$=7.3 MHz. The series resistance originates an increase of C'' with slope 1 in a log–log scale reaching the maximum amplitude ($C'_{\mathrm{hf}}/2 = 2.18$ nF) at 7.3 MHz. This contribution becomes observable below 1 MHz due to the low C'' values of the junction capacitance. On the other hand the effect of this series resistance on C' consists of a decrease toward zero beyond the relaxation frequency with slope -2 in a log–log scale. However, in a Debye relaxation C' changes slightly below the relaxation frequency: An easy calculation using the expression of the frequency dependence of the capacitance quoted above shows that a relative change of only 1% occurs in the real part of the capacitance one decade below the relaxation frequency. This explains the relatively flat C' characteristic for frequencies up to 0.8 MHz. In this way a C'' characteristic free from the effect of the series resistance can be obtained by KK transforming the measured C' data up to 0.8 MHz (see Fig. 6). This improves largely the accuracy in determining the position and the amplitude of the deep level related peak otherwise distorted by the effect of the series resistance. As can be seen from this figure, the position of the peak is clearly shifted for the transformed data. It has to be emphasized that the temperature activated series resistance may have a significant effect in an accurate determination of the position of the peak when temperature is changed, thus yielding erroneous level positions. At temperatures above 320 K the effect of the shunt conductance becomes dominant at low frequencies distorting the C'' peak. KK transformations allow obtaining the C'' associated with the deep level free of the effect of R_s and G_0. Figure 7(a) shows the measured C' data at different temperatures. Figure 7(b) shows the C'' data obtained from C' at these same temperatures. An energy level of 0.54 eV has been obtained from the shift of the peak toward low frequencies when temperature is lowered. An Arrhenius plot of the peak frequency versus the reciprocal temperature is shown in Fig. 7(b) as an inset. It is interesting to note that a complex nonlinear least-squares fitting to a response model would be a more adequate procedure to separate junction admittance from the effect of series and shunt resistance,[4–6] however, this response model is not known in our case in which the junction response is affected

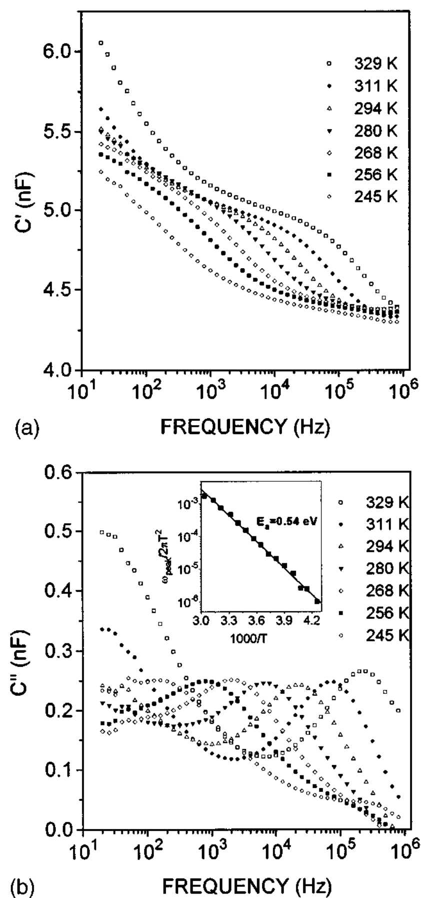

FIG. 7. (a) C' for a CdS/CdTe heterojunction measured at different temperatures. (b) C'' data obtained by KK transforms from the C' data shown in (a). An Arrhenius plot of $\log(\omega_p/2\pi T^2)$ is shown as an inset in (b).

by a not known distribution of interface states (probably caused by lattice mismatch) through which excess charge carriers recombine.

V. CONCLUSIONS

The use of Kramers–Kronig transforms on measured data has shown to be useful to accomplish AS characterization of junctions with significant shunt or series resistance. An algorithm has been developed to calculate numerically the KK transforms, which allows evaluating the imaginary part of the complex capacitance from the real one, not affected by shunt conductance. This algorithm has been tested using simulated data for two systems, one showing a Debye-like relaxation, and the other one a Cole–Cole relaxation in the complex capacitance.

This method has also been applied to p-n junctions into InP made by ion implantation, in which the shunt conductance overshadowed the presence of peaks in C'' related to deep levels. Using KK relations the peaks appeared clearly showing two different deep levels with activation energies of 0.2 and 0.35 eV. The level at 0.35 eV is probably related to the implantation damage as it disappeared after annealing the samples for 10 s instead of 5 s. ALE-grown CdS/CdTe solar cells have also been analyzed with this procedure due to the presence of both shunt conductance and series resistance on the measured C'' and showed a single trap level at 0.54 eV.

[1] D. L. Losee, J. Appl. Phys. **46**, 2204 (1975).
[2] J. L. Pautrat, B. Katircioglu, N. Magnea, J. C. Pfister, and L. Revoil, Solid-State Electron. **23**, 1159 (1980).
[3] C. Ghezzi, Appl. Phys. A **23**, 191 (1981).
[4] *Impedance Spectroscopy—Emphasizing Solid Materials and Systems*, edited by J. R. Macdonald (Wiley-Interscience, New York, 1987).
[5] B. A. Boukamp and J. R. Macdonald, Solid State Ionics **74**, 85 (1994).
[6] J. R. Macdonald, J. Chem. Phys. **102**, 6241 (1995).
[7] B. A. Boukamp, Solid State Ionics **62**, 131 (1993).
[8] M. Urquidi-Macdonald, S. Real, and D. D. Macdonald, Electrochim. Acta **35**, 1559 (1990).
[9] J. R. Macdonald, Electrochim. Acta **38**, 1883 (1993).
[10] A. K. Jonscher, *Dielectric Relaxation in Solids* (Chelsea Dielectric, London, 1983).
[11] R. Wooldridge, *An Introduction to Computing* (Oxford University Press, London, 1962).
[12] B. A. Boukamp, J. Electrochem. Soc. **142**, 1885 (1995).
[13] J. M. Martin, S. García, F. Calle, I. Mártil, and G. González-Díaz, J. Electron. Mater. **24**, 59 (1995).
[14] M. W. Focht, A. T. Macrander, B. Schwartz, and L. C. Feldman, J. Appl. Phys. **55**, 3859 (1984).
[15] J. Skarp, Y. Koskinen, S. Lindfors, A. Rautiainen, and T. Suntola, in Proceedings of the 10th European Photovoltaic Solar Energy Conference Lisbon, Portugal, April 8–12, 1991, p. 567.
[16] J. Skarp, E. Anttila, A. Rautiainen, and T. Suntola, Int. J. Sol. Energy **12**, 137 (1992).
[17] S. J. Pearton, C. R. Abernathy, M. B. Panish, R. A. Hamm, and L. M. Lunardi, J. Appl. Phys. **66**, 656 (1989).

Journal of Applied Physics is copyrighted by the American Institute of Physics (AIP). Redistribution of journal material is subject to the AIP online journal license and/or AIP copyright. For more information, see http://ojps.aip.org/japo/japcr/jsp
Copyright of Journal of Applied Physics is the property of American Institute of Physics and its content may not be copied or emailed to multiple sites or posted to a listserv without the copyright holder's express written permission. However, users may print, download, or email articles for individual use.

Journal of Applied Physics is copyrighted by the American Institute of Physics (AIP). Redistribution of journal material is subject to the AIP online journal license and/or AIP copyright. For more information, see http://ojps.aip.org/japo/japcr/jsp